All-Optical ACP-OPLL Photonic Integrated Circuit

Y. Li[+], A. Bhardwaj[#], R. Wang[+], S. Jin[+], L. Coldren[#], J. Bowers[#], and P. Herczfeld[*]

[+]University of Massachusetts at Dartmouth, MA 02747, USA
[*]Drexel University, Philadelphia, PA 19104, USA
[#]The University of California, Santa Barbara, CA 93101, USA

***Abstract* — The optical-phase-locked-loop linear phase demodulator is the most critical component for a high dynamic range phase modulated RF/Photonic link. Due to the stringent loop latency requirement, the OPLL should be implemented as a photonic integrated circuit. In this paper we address the design and implementation of an all optical attenuation-counter-propagating (ACP) optical-phase-locked-loop photonic integrated circuit. The preliminary experimental results for this device are also presented.**

***Index Terms* — Optical phase locked loop, photonic integrated circuits, dynamic range.**

I. INTRODUCTION

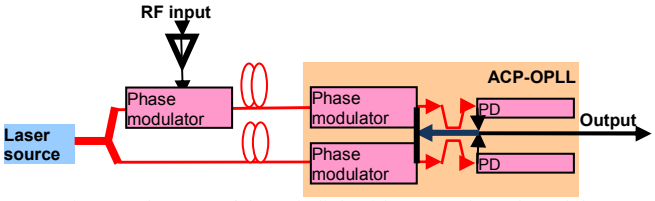

Fig. 1: Coherent RF/photonic link with OPLL phase demodulator

An RF/Photonic link for radar frontend applications requires a large Spurious-Free Dynamic Range (SFDR). However, conventional fiber-optic links that employ intensity modulation and direct detection (IM-DD) have limited SFDR due to the nonlinearities in the optical modulation process. As a solution, we have proposed a coherent phase modulated RF/photonic link shown in Fig. 1[1-2]. The most critical element in this link is an Optical Phase-Locked Loop (OPLL) linear phase demodulator. Through feedback, the OPLL forces the output phase of a local optical phase modulator to mirror the phase of an incoming optical signal. Thus, the output from the photodetectors of the OPLL is a scaled replica of the RF input at the link transmitter. In order to tightly track the phase optical carrier, the OPLL must have a high open loop gain (~20 dB) and a wide bandwidth (>0.5 GHz). Thus, feedback stability requires that the OPLL has an extremely short loop propagation delay (<10 ps). To realize the delay requirement, the attenuation counter-propagating (ACP) device design was proposed [3], which renders a lumped-element low-pass response to both the optical phase modulators and the photodetectors inside the OPLL. However, to further reduce the loop delay, the OPLL should also be integrated on a chip in order to minimize the propagation delays arising from signal routing and feedback. In this paper, we describe the design and implementation of an ACP-OPLL Photonic Integrated Circuit (PIC) on an Indium Phosphide (InP)-based material platform, and present some preliminary experimental results.

II. ACP-OPLL PIC DESIGN

The first major problem facing the design of the ACP-OPLL PIC is the nonlinearity of the quantum well optical phase modulators. We have developed and experimentally verified a detuned shallow MQW phase modulator with record linearity and low optical propagation loss [4]. The quantum well design consists of lattice matched 9 nm thick $In_{0.65}Ga_{0.35}As_{0.76}P_{0.24}$ quantum wells and 6.5 nm thick $In_{0.8}Ga_{0.2}As_{0.44}P_{0.56}$ barriers. We use this quantum well design to implement the ACP phase modulators inside the OPLL photonic integrated circuit.

As shown in Fig. 2, our ACP-OPLL photonic integrated circuit contains:

- 3 mm long push-pull balanced ACP-phase modulators
- 200 microns long balanced counter-propagating photodetectors
- A 217 microns long regular interference MMI coupler

Table 1 summarized the design of the ACP-OPLL PIC.

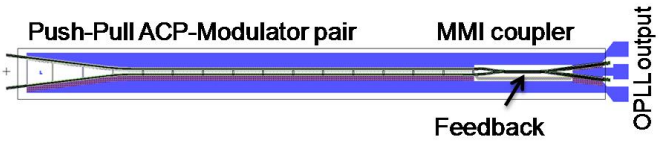

Fig. 2: ACP-OPLL Mask layout

Table 1 ACP-OPLL PIC design parameters

ACP modulator length	3 mm
ACP modulator V_π	~2 volt
ACP modulator loss	<3dB
MMI coupler Length	217 μm
Photodetector length	200 μm
PD 95%absorption length	168μm
Loop delay	~10ps

A. Push-pull ACP phase modulator

The key idea of the ACP phase modulator is to use the RF attenuation to synthesize a lumped element low-pass response [3]. We use a high resistance thin film electrode to introduce the desired RF attenuation to the phase modulator electrode.

978-1-61284-757-3/11/$26.00 C2011 IEEE

However, this can create non-uniform bias voltage along the quntum well phase modulators. When under optical input, a substantial photocurrent (>1mA) is generated [4]. When this photocurrent flows through the lossy electrode, it can cause an unwanted bias voltage variation along the length of the electrode. A constant bias voltage is critical for the phase modulator's lineairty. To mitigate this effect, we have developed a push-pull ACP phase modulator pair as illustrated in Fig. 3.

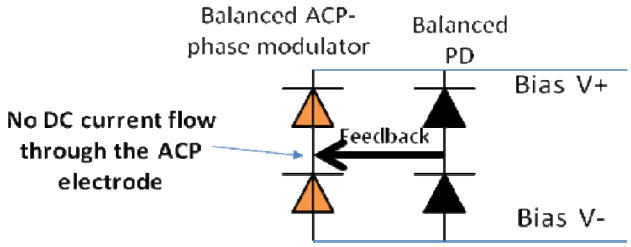

Fig. 3:Push-pull balanced ACP phase modulator and balanced Pd

In this design the photocurrents generated in each ACP-phase modulator complement each other. Thereby, there is no net DC photocurrent flowing through the high resistance ACP thin film electrode. The optimum bias voltage is maintained throughout the ACP electrode. This push-pull modulator design also doubles the open-loop gain, which is very beneficial when the optical power that couples into the photodetector is low.

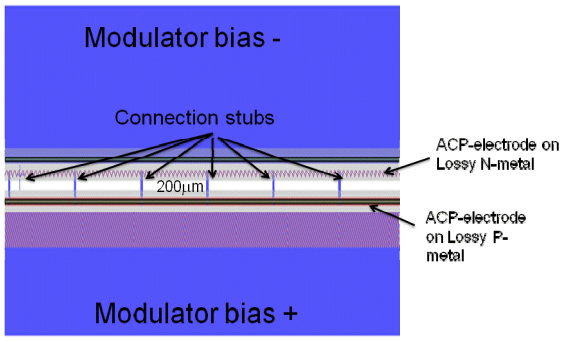

Fig. 4 A secion of push-pull ACP phase modulator

A section of the photomask layout of the push-pull ACP phase modulator is shown in Fig. 4. The lossy electrodes of the upper and the lower ACP-modulators are implemented on modulator lossy-n-metal and lossy-p-metal layers, respectively. Both electrodes has a resistance of approximately 150ohm.

The lossy metal recipe tailors the RF loss to be small within the OPLL bandwidth and large beyond this bandwidth. This eliminates the modulator's propagation delay without sacrificing too much the modulation sensitivity and linearity within the OPLL bandwidth. The simulated effective V_π of the push-pull ACP phase modulator pair is ~1 volt. Also shown in Fig. 9, the two lossy electrodes are electrically connected by an array of 3 micron wide metal stubs. The distance between the adjacent stubs is 200 microns. The unwanted RF reflection due to these stubs was carefully simulated using Ansoft HFSS. It was found to be small and does not reduce the OPLL phase margin.

B. Balanced counter propagating balanced UTC PD

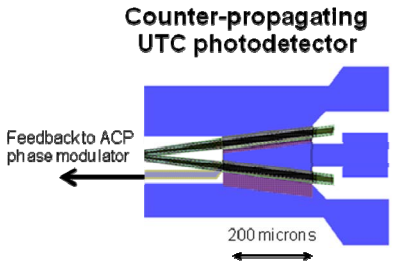

Fig. 5: Counter propagating balanced UTC photodetector

The photodetector (Fig 5) is based on a waveguide Uni-travelling Carrier Photodiode (UTC-photodetector) design [5]. In order to minimize the delay, we introduce a counter-propagating photodetector configuration. The detector width and length are 10 microns and 200 microns, respectively. The photodetector's absorption length is 168 microns. Each photodetector is capable of achieving a saturation photocurrent >50mA.

C. 3dB optical coupler

To mitigate risks, a regular multi-mode interferometric (MMI) coupler was used to implement the 3dB coupler (Fig. 6). The length of the coupler is 217 microns. Its loss was simulated to be less than 0.3dB. The MMI coupler sets the total OPLL loop delay to be ~10ps, which includes delays of the MMI coupler, waveguide bends, tapers and feedback electrode. By employing more compact couplers, much shorter delay can be achieved.

Fig. 6. Regular MMI 3dB coupler (217 micron long and 7 micron wide)

Table 2 Simulated ACP-OPLL performance

Photocurrent	~45 mA/PD
Load impedance	50 ohm
SFDR in shot noise limit	~140 dB*Hz$^{2/3}$
Open loop gain	~22 dB
Bandwidth	~0.7 GHz
Phase Margin	60 degrees

D. ACP-OPLL PIC performance projection

978-1-61284-757-3/11/$26.00 C2011 IEEE

The ACP-OPLL PIC design was simulated and its performance with 45 mA photocurrent is summarized in Table 3. In the calculation, we assume the shot-noise limit.

III. Experimental Results

The ACP-OPLL PIC was fabricated using UCSB's nanofabrication facilities. The base epitaxially grown wafer for the fabrication of the ACP-OPLL PIC was provided by Landmark Inc. It contains the MQW layers for the phase modulators as well as the layers for the UTC-photodetector on a semi-insulating InP substrate. The layers that define the UTC photodetector were first removed selectively for the regions where the detector is not present. Then the p-contact layers were regrown. Deep ridge optical waveguides were defined, followed by n-metal deposition. Helium implantation and proton implantation were performed to introduce electric isolation between the loop components. Finally, the p-metal deposition was performed. The details on the fabrication steps will be addressed in a separate paper. Fig. 7 shows a group of three ACP-OPLL PICs mounted on a carrier chip.

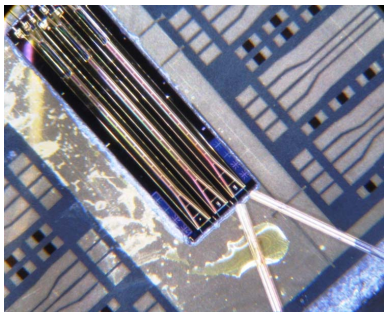

Fig. 7 Fabricated ACP-OPLL PICs

A. Phase modulator optical loss

To realize the full dynamic range potential of the ACP-OPLL PIC, it is critical to generate large photocurrents from the balanced photodetectors of the ACP-OPLL. This requires that the ACP phase modulators have low optical loss. A dual drive modulator test structure device (as shown Fig. 8) was co-fabricated with the ACP-OPLLs. It was used to determine the optical loss of the ACP phase modulators.

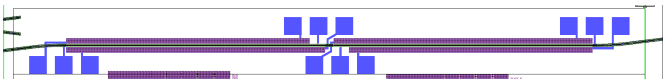

Fig. 8. Dual drive phase modulator test structure

The dual drive modulator contains two identical 1.5 mm long modulator sections, which are reverse based and used as a photodetector instead. The modulator optical loss is determined by comparing the ratio between the photocurrents of the two modulator sections when illuminated by a small optical input. The measured optical loss (Fig. 9) for a 1.5 mm long modulator section is ~3 dB, suggesting an optical absorption of ~2 dB/mm. It does not show strong dependence on the modulator bias and optical input power.

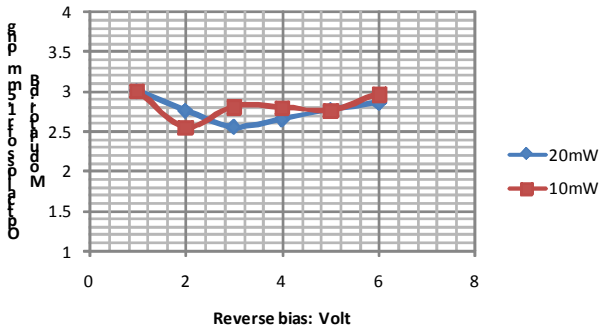

Fig. 9 Phase modulator optical loss measurement results

B. Preliminary ACP-OPLL PIC characterization

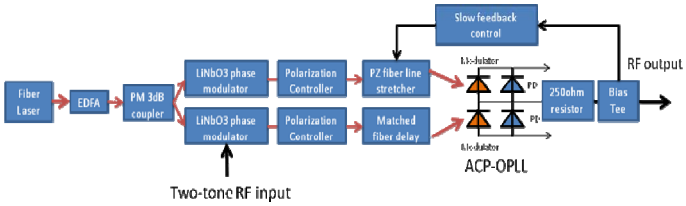

Fig. 10. PM link experiemental setup

The ACP-OPLL PIC is characterized using the setup shown in Fig. 10. It is a phase modulated optical link. A 1.55micron CW low phase-noise fiber laser provides the optical carrier. The output of the fiber laser is amplified using a high power erbium doped fiber amplifier, and then split into two paths using a polarization maintaining 3 dB optical coupler. Each path contains a $LiNbO_3$ linear phase modulator (V_π~7volt), which is used as the link transmitter. After some fiber delay, the two paths are recombined at the ACP-OPLL PIC, in order to perform linear phase demodulation. In addition, to overcome the slow environmental fluctuations of the relative optical phase between the two optical paths, the low frequency portion (<100 kHz) of the ACP-OPLL output is extracted via a microwave bias-Tee and is fed back to a Piezo-electric fiber line stretcher. This slow feedback allows long-term stable phase locking.

In this preliminary experiment we generate ~4 mA photocurrent in each photodetector of the ACP-OPLL PIC. To increase the ACP-OPLL open loop gain in presence of the low photocurrent, a 250 ohm series resistor was placed between the ACP-OPLL output and the external 50 ohm load. This elevates the load impedance of the ACP-OPLL output to 300 ohm.

To establish the baseline for comparison, we first "turn off" the optical feedback by intentionally reducing the photocurrent to a negligible level so that the OPLL open loop gain is close to zero. Thereby, the ACP-OPLL is reduced to a conventional homodyne phase detector. Fig. 11 shows the output captured by a microwave spectrum analyzer when the two-tone RF input is at 100 MHz and 12 dBm per tone. The measured inter-modulation distortion is ~29dBc.

978-1-61284-757-3/11/$26.00 C2011 IEEE

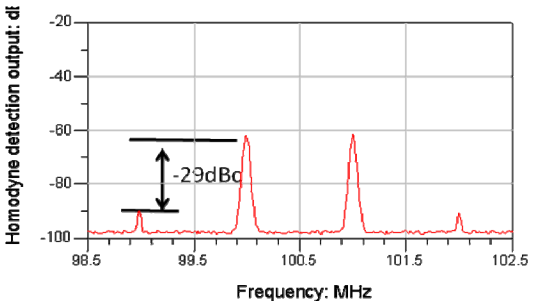

Fig. 11 Distortion level of homodyne phase detector without feedback

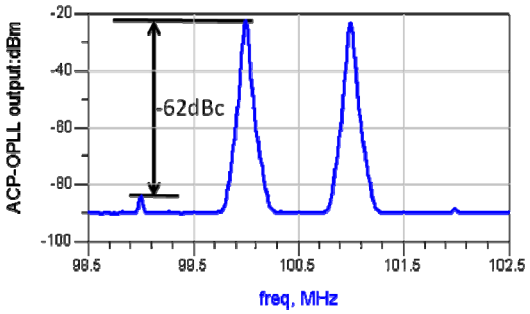

Fig. 12 Distortion of ACP-OPLL. 33dB improved in distortion level is observed. The photocurrent is 4mA and the rest input condition is similar to that of Fig.11.

Under the same RF input condition, we increased the optical input power to obtain ~4 mA photocurrent from each photodetector. With the OPLL feedback enabled, we observed a 33 dB reduction in the intermodulation distortion (IMD) levels as shown in Fig. 12. The distortion level in this measurement is very close to the spectrum analyzer's noise floor and the 12 dBm/tone RF input power is the power limit of the RF signal sources. Thus, we are unable to determine the distrotion level as a function of the RF input power under these conditions.

IV. Conclusions

We have described the design, implementation of the ACP-OPLL PICs and have presented results from preliminary measurements. With only 4 mA photocurrent, we obtained 33 dB improvement in spurious distortion levels.

Acknowledgement

The authors wish to acknowledge Dr. Leif Johansson, Dr. Arye Rosen, and Dr. Jonathan Klamkin for valuable suggestions.

References

[1] Y. Li, P. Herczfeld, "Coherent PM optical link employing ACP-PPLL", *OSA/IEEE Journal of Lightwave Technology*, vol. 27, no. 9, May 2009, pp. 1086-1094.

[2] J. E. Bowers, A. Ramaswamy, L.A. Johansson, J. Klamkin, M.N. Sysak, D.Zibar, L.A. Coldren, M.J. Rodwell, L. Lembo, R. Yoshimitsu, D. Scott, R. Davis, P. Ly, "Linear Coherent Receiver based on a Broadband and Sampling Optical Phase-Locked Loop," *Microwave Photonics '07 (Invited),* Victoria, Canada, OCTOBER 2007

[3] Y. Li, P. Herczfeld, "Novel attenuation counter propagating phase modulator for highly linear fiber optic links", *OSA/IEEE Journal of Lightwave Technology*, Oct., 2006

[4] Y. Li, R. Wang, A. Bhardwaj, S. Ristic and J. Bowers, "High linearity InP based phase modulators using a Shallow Quantum well Design", *IEEE Photonic Technology Letter*, vol 22, no. 18, 2010, pp 1340-1342

[5] J. Klamkin, et al, "Output Saturation and Linearity of Waveguide Unitraveling-Carrier Photodiodes," *IEEE Journal of Quantum Electronics*, 44, (4), pp. 354-359, April 2008